

See discussions, stats, and author profiles for this publication at: <https://www.researchgate.net/publication/225294697>

# ESI-MS Studies of the Dehydrogenative Heck Reaction of Furans with Acrylates Using Benzoquinone as the Reoxidant and DMSO as the Solvent

ARTICLE *in* THE JOURNAL OF ORGANIC CHEMISTRY · JUNE 2012

Impact Factor: 4.72 · DOI: 10.1021/jo300921s · Source: PubMed

---

CITATIONS

18

---

READS

18

## 4 AUTHORS, INCLUDING:



**Dominique Harakat**

French National Centre for Scientific Research

103 PUBLICATIONS 647 CITATIONS

SEE PROFILE



**Jacques Muzart**

French National Centre for Scientific Research

318 PUBLICATIONS 5,915 CITATIONS

SEE PROFILE



**Jean Le Bras**

Université de Reims Champagne-Ardenne

83 PUBLICATIONS 1,554 CITATIONS

SEE PROFILE

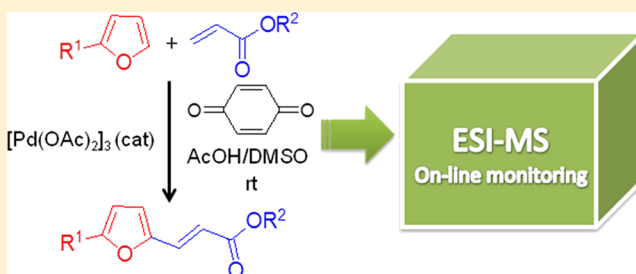
# ESI-MS Studies of the Dehydrogenative Heck Reaction of Furans with Acrylates Using Benzoquinone as the Reoxidant and DMSO as the Solvent

Alexandre Vasseur, Dominique Harakat, Jacques Muzart, and Jean Le Bras\*

Institut de Chimie Moléculaire de Reims-UMR 7312 CNRS-Université de Reims Champagne-Ardenne UFR des Sciences Exactes et Naturelles, BP 1039, 51687 REIMS Cedex 2, France

## S Supporting Information

**ABSTRACT:** Electrospray ionization mass spectrometry, subsequent MS/MS, and high-resolution mass spectrometry were used to study the dehydrogenative Heck reaction of 2-alkylfurans **1** with acrylates **2**, using  $[\text{Pd}(\text{OAc})_2]_3$  as the precatalyst, benzoquinone (BQ) as the stoichiometric oxidant, and a mixture of DMSO and AcOH as the solvent. Complexation of  $[\text{Pd}(\text{OAc})_2]_3$  by DMSO afforded mononuclear and dinuclear Pd(II) species, which proved to be active catalysts for the C–H activation of **1**. Mononuclear and dinuclear Pd(II) species seem also to be involved in the insertion of **2** into the furyl–Pd bond. The C–H activation of **2** and DMSO by mononuclear complexes was observed. The reaction leads to 5,5'-dialkyl-2,2'-bifuran **4** as a byproduct. Bifuryl-palladium, which is an intermediate in the formation of **4**, showing the coordination of BQ, was obtained and characterized.



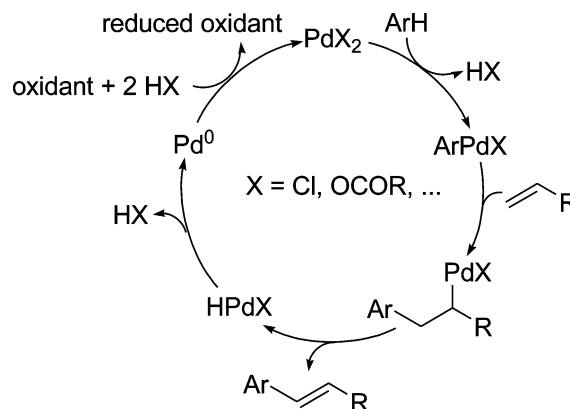
## INTRODUCTION

The Pd-catalyzed direct cross-couplings of arenes with alkenes through C–H activation, also called intermolecular dehydrogenative Heck reactions (DHRs), have drawn much attention.<sup>1</sup> These transformations are of interest in terms of atom economy, since the result of the DHRs is the formation of a C–C bond from two C–H bonds. Previous research has focused on the use of electron-rich alkenes,<sup>2</sup> new promoters,<sup>3</sup> the development of cascade,<sup>4</sup> enantioselective,<sup>5</sup> diastereoselective,<sup>6</sup> and regioselective reactions.<sup>7</sup> The mechanism of such transformations has been studied by standard approaches such as kinetics and the use of labeled compounds.<sup>1</sup> This research involves the C–H activation of the arene to provide an  $\text{ArPd}(\text{II})\text{X}$  species, followed by the insertion of the alkene into the Ar–Pd bond (Scheme 1). A  $\beta$ -H elimination leads to the product and  $\text{HPdX}$ . Usually, the latter evolves to  $\text{Pd}(0)$  which is then reoxidized.

Electrospray ionization mass spectrometry (ESI-MS) is well adapted for the observation of protonated, deprotonated, or cationized forms of short-lived molecules produced by catalyzed reactions. The technique, thus, provides continuous snapshots of the composition of the reaction solution and hence insights into its mechanism.<sup>8</sup> For example, the online monitoring of the Heck<sup>9a</sup> and Baylis-Hillman<sup>9b</sup> reactions has allowed the characterization of several catalytic intermediates. Dynamic and time-dependent processes were also observed using such a technique. Since these original studies, others, on a variety of catalytic transformations, have been reported.<sup>10</sup>

Our initial findings on the DHR of furans have shown that the solvent can have a decisive influence on the course of the

Scheme 1. Typical Mechanism for Dehydrogenative Heck Reactions

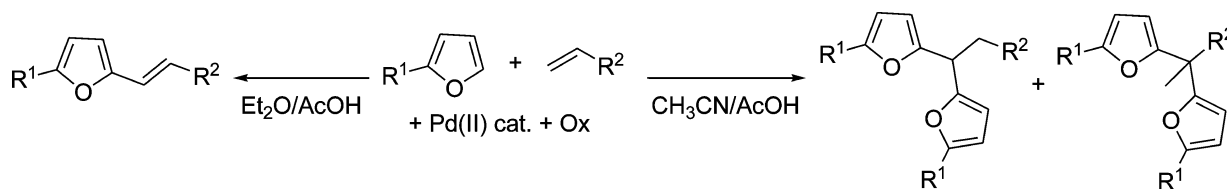


reaction. Low-coordinating solvents led to Heck-type products,<sup>11</sup> whereas coordinating solvents gave difurylalkanes (Scheme 2).<sup>12</sup> We have recently observed that DMSO, which is a coordinating solvent,<sup>13</sup> allowed the formation of Heck-type products through the coupling of furans and thiophenes with alkenes, under mild conditions.<sup>14</sup> This surprising result prompted us to study the mechanism of these reactions using ESI-MS.

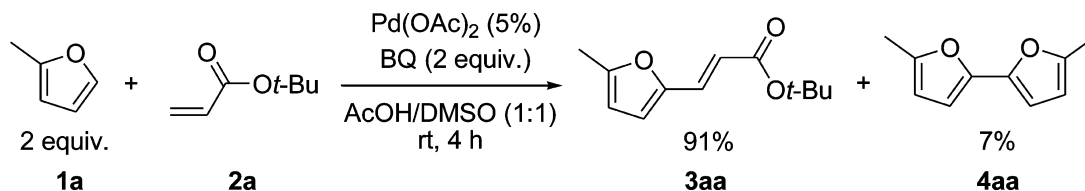
Received: May 7, 2012

Published: June 12, 2012

Scheme 2. Solvent Effect in the DHR of Furans



Scheme 3. Reaction Studied by ESI-MS



## RESULTS AND DISCUSSION

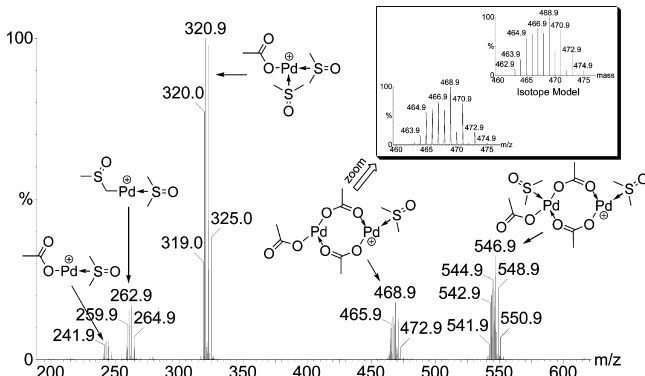
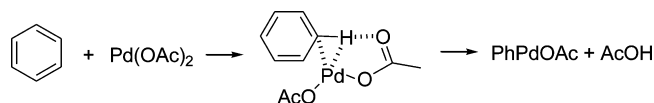
Since ionization efficiency under ESI-MS conditions depends on the polarity of the molecule, we have selected acrylates as alkenes for the DHR of furans. The reaction of 2-methylfuran (**1a**) and *tert*-butyl acrylate (**2a**) in the presence of  $\text{Pd}(\text{OAc})_2$  (5%) and benzoquinone (BQ), in a mixture of AcOH and DMSO at room temperature for 4 h, led to the Heck-type product **3aa** and 5,5'-dimethyl-2,2'-bifuran (**4aa**) with yields of 91% and 7%, respectively (Scheme 3).

Using ESI(+)-MS, we have first monitored a mixture of  $\text{Pd}(\text{OAc})_2$  and BQ in AcOH/DMSO (1:1), and after 5 min of stirring, five clusters were detected (Figure 1, Figure S1 of the

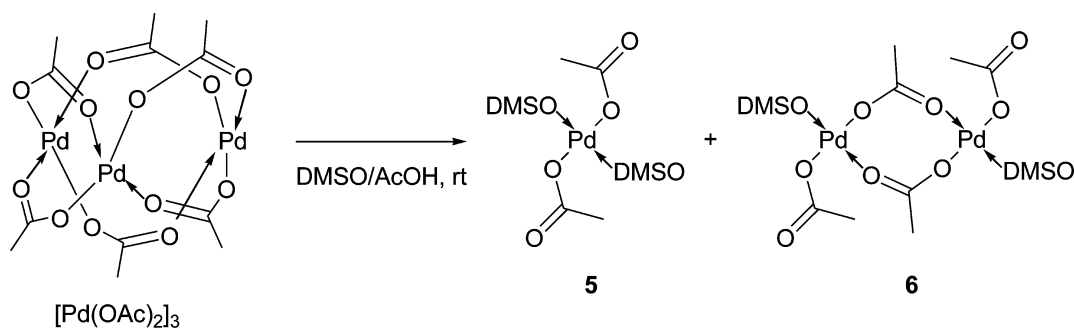
Supporting Information).  $[\text{Pd}(\text{OAc})(\text{DMSO})]^+$  and  $[\text{Pd}(\text{OAc})(\text{DMSO})_2]^+$ , observed at  $m/z$  242.9 and 320.9, respectively, originated from the solvated species,  $\text{Pd}(\text{OAc})_2 \cdot (\text{DMSO})_2$ . The dinuclear analogue  $\text{Pd}_2(\text{OAc})_4(\text{DMSO})_2$  was observed as  $[\text{Pd}_2(\text{OAc})_3(\text{DMSO})]^+$  and  $[\text{Pd}_2(\text{OAc})_3(\text{DMSO})_2]^+$  at  $m/z$  466.9 and 544.9, respectively.

Palladium acetate exists as a trimer in the solid state,<sup>15</sup> and this structure is maintained in AcOH.<sup>16</sup> As shown from the ESI(+)-MS study, the use of DMSO as cosolvent led to the formation of mononuclear and dinuclear species **5** and **6**, respectively (Scheme 4).

Davies and Macgregor, in a recent review on computational studies of metal-induced C–H bond activations, assumed that the  $\text{Pd}(\text{OAc})_2$ -mediated activation of benzene was assisted by the acetate ligand (Scheme 5).<sup>17</sup>

Scheme 5. C–H Activation of Benzene by  $\text{Pd}(\text{OAc})_2$ 

**Figure 1.** ESI(+)-MS of an AcOH/DMSO solution of  $\text{Pd}(\text{OAc})_2$  and BQ after 5 min. Conditions:  $\text{Pd}(\text{OAc})_2$  (0.05 mmol), BQ (2.0 mmol), AcOH (2.0 mL), and DMSO (2.0 mL).  $t_R$  = 5 min.

Scheme 4. Formation of **5** and **6**

$[\text{Pd}(\text{OAc})_2]_3$  by electron-rich furans probably leading to dimeric or monomeric Pd-active species.<sup>11</sup> In contrast, no induction period was observed in the solvent mixture of DMSO/AcOH<sup>14</sup> since DMSO acts as a ligand, thus leading to active species **5** and **6**, which can both participate in the DHR.<sup>18</sup> The observation of the cluster  $[\text{Pd}(\text{DMSO-H})(\text{DMSO})]^+$  at  $m/z$  260.9 (Figure 1, Figure S1 of the Supporting Information) suggests that **5** can also activate a  $\text{C}(\text{sp}^3)\text{-H}$  bond of DMSO.

All structures shown in Figure 1 were confirmed by high-resolution mass spectrometry (HRMS) analysis. In addition, when  $\text{CD}_3\text{CO}_2\text{D}$  was used instead of AcOH, clusters were shifted by 3 or 9 mass units depending on the number of acetate ligands (Table 1, Figure S2 of the Supporting

**Table 1.** Comparison of Detected Species Using AcOH,  $\text{CD}_3\text{CO}_2\text{D}$ , or  $\text{DMSO-d}_6$

proposed structures	$m/z$ observed in		
	AcOH/ DMSO	$\text{CD}_3\text{CO}_2\text{D}$ / DMSO	AcOH/ DMSO- $\text{d}_6$
$[\text{Pd}(\text{OAc})(\text{DMSO})]^+$	242.9	246.0	248.9
$[\text{Pd}(\text{DMSO-H})(\text{DMSO})]^+$	260.9	261.0	272.0
$[\text{Pd}(\text{OAc})(\text{DMSO})_2]^+$	320.9	324.0	333.0
$[\text{Pd}_2(\text{OAc})_3(\text{DMSO})]^+$	466.9	476.0	474.9
$[\text{Pd}_2(\text{OAc})_3(\text{DMSO})_2]^+$	544.9	554.0	558.9

Information). A new cluster observed at  $m/z$  488.1 was attributed to the solvated species,  $[\text{Pd}(\text{DMSO})_4(\text{CD}_3\text{CO}_2)]^+$ . The presence of DMSO in the proposed structures was confirmed using DMSO- $\text{d}_6$  (Table 1, Figure S3 of the Supporting Information).

Using ESI(+)-MS, we then monitored a mixture of  $\text{Pd}(\text{OAc})_2$ , BQ, and **1a** in AcOH/DMSO (1:1). After 5 min of stirring, new clusters were detected and most of them could be identified (Figure 2, Figure S4 of the Supporting

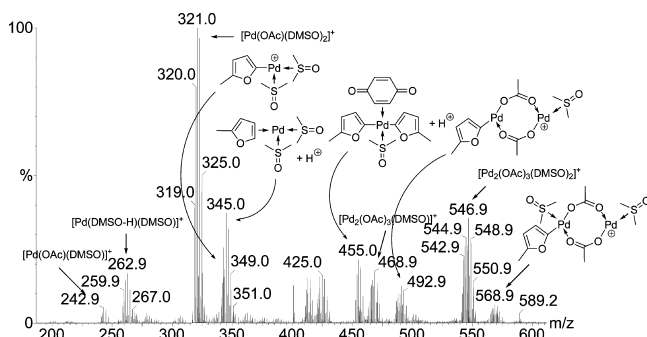


**Figure 2.** ESI(+)-MS of an AcOH/DMSO solution of **1a**,  $\text{Pd}(\text{OAc})_2$ , and BQ after 5 min. Conditions: **1a** (2.0 mmol),  $\text{Pd}(\text{OAc})_2$  (0.05 mmol), BQ (2.0 mmol), AcOH (2.0 mL), and DMSO (2.0 mL).  $t_R$  = 5 min.

Information).  $[\text{Pd}(\text{1a-H})(\text{DMSO})_2]^+$  of  $m/z$  343.0 originated from the C–H activation of **1a** by **5**, while  $[\text{Pd}_2(\text{1a-H})(\text{OAc})_2(\text{DMSO})]^+$  of  $m/z$  488.9 and  $[\text{Pd}_2(\text{1a-H})(\text{OAc})_2(\text{DMSO})_2]^+$  of  $m/z$  566.9 resulted from the C–H activation of **1a** by **6**. Such complexes, which are connected to neutral species,  $\text{Pd}(\text{1a-H})(\text{OAc})(\text{DMSO})_2$  and  $\text{Pd}_2(\text{1a-H})(\text{OAc})_3(\text{DMSO})_2$ , suggest that mononuclear and dinuclear species are involved in the first step of the DHR. The cluster observed at  $m/z$  345.0 was attributed to  $[\text{Pd}(\text{1a})(\text{DMSO})_2\text{H}]^+$

(Figure 2, Figure S4 of the Supporting Information) and corresponds to the protonated form of the Pd(0) complex,  $\text{Pd}(\text{1a})(\text{DMSO})_2$ . Pd(0) can come from the formation of **4aa**, but the close similarity between both structures,  $\text{Pd}(\text{1a-H})(\text{OAc})(\text{DMSO})_2$  and  $\text{Pd}(\text{1a})(\text{DMSO})_2$ , also suggests that the latter could be obtained by the reduction of the former via electrochemical processes occurring in the electrospray process.<sup>19</sup> However, this phenomenon is probably not significant because such a relationship was not observed for other clusters. The ESI(+)-MS/MS data of  $[\text{Pd}(\text{1a-H})(\text{DMSO})_2]^+$  and  $[\text{Pd}(\text{1a})(\text{DMSO})_2\text{H}]^+$  are quite similar (Table 2, Figures S5 and S6 of the Supporting Information).

**Table 2.** ESI(+)-MS/MS of Detected Species with a Solution of  $\text{Pd}(\text{OAc})_2$ , BQ, and **1a** in AcOH/DMSO

proposed structures	losses
$[\text{Pd}(\text{1a-H})(\text{DMSO})_2]^+$	DMSO, <b>1a</b>
$[\text{Pd}(\text{1a})(\text{DMSO})_2\text{H}]^+$	DMSO, <b>1a</b>
$[\text{Pd}_2(\text{1a-H})(\text{OAc})_2(\text{DMSO})]^+$	DMSO, AcOH, Pd
$[\text{Pd}_2(\text{1a-H})(\text{OAc})_2(\text{DMSO})_2]^+$	DMSO, AcOH, Pd
$[\text{Pd}(\text{1a-H})_2(\text{BQ})(\text{DMSO})\text{H}]^+$	DMSO, BQ, Pd

The elimination of **1a** in the MS/MS of  $[\text{Pd}(\text{1a-H})(\text{DMSO})_2]^+$  is quite surprising, but this observation is probably due to the superposition of the signal with the one from the Pd(0) analogue  $[\text{Pd}(\text{1a})(\text{DMSO})_2\text{H}]^+$  in which **1a** would be coordinated as a  $\pi$ -ligand. The ESI(+)-MS/MS data of dinuclear species,  $[\text{Pd}_2(\text{1a-H})(\text{OAc})_2(\text{DMSO})]^+$  and  $[\text{Pd}_2(\text{1a-H})(\text{OAc})_2(\text{DMSO})_2]^+$ , were similar and showed the losses of DMSO, AcOH, and Pd (Table 2, Figures S7 and S8 of the Supporting Information). The loss of the organic acid was confirmed when  $\text{CD}_3\text{CO}_2\text{D}$  was used as the solvent.<sup>20</sup>

The cluster detected at  $m/z$  455.0 was attributed to  $[\text{Pd}(\text{1a-H})_2(\text{BQ})(\text{DMSO})\text{H}]^+$  (Figure 2, Figure S4 of the Supporting Information). Such a species corresponds to the protonated form of  $\text{Pd}(\text{1a-H})_2(\text{BQ})(\text{DMSO})$  which could be an intermediate in the formation of **4aa**. Indeed, it has been proposed that BQ induces reductive elimination in various palladium-catalyzed transformations.<sup>21</sup> It must be noted that we did not observe any traces of **4aa** when the coupling of **1a** with **2a** was performed in  $\text{CH}_3\text{CN}$ .<sup>12</sup> Nevertheless, the bifuryl complex  $[\text{Pd}(\text{1a-H})_2]^+$  was observed by ESI(+)-MS, but no BQ adduct was detected; the coordinating solvent  $\text{CH}_3\text{CN}$  probably prevents the complexation of BQ and, hence, the reductive elimination.  $[\text{Pd}(\text{1a-H})_2(\text{BQ})(\text{DMSO})\text{H}]^+$  dissociated to produce DMSO, BQ, and Pd (Table 2, Figure S9 of the Supporting Information). The latter is a fragmentation that is known to occur through reductive elimination of the  $\text{R}_2\text{Pd}$  species.<sup>22</sup> The loss of BQ confirms its coordination to palladium. Since we never observed such an interaction by ESI-MS in other oxidative palladium reactions,<sup>12,23</sup> and in order to confirm the presence of BQ, we have monitored a mixture of  $\text{Pd}(\text{OAc})_2$ , chlorobenzoquinone (Cl-BQ), and 2-ethylfuran (**1b**), in AcOH/DMSO (1:1) using ESI(+)-MS. After 5 min of stirring, the expected cluster  $[\text{Pd}(\text{1b-H})_2(\text{Cl-BQ})(\text{DMSO})\text{H}]^+$  was observed at  $m/z$  517.1; its structure was confirmed by HRMS. The desolvated complex  $[\text{Pd}(\text{1b-H})_2(\text{Cl-BQ})\text{H}]^+$  was also detected at  $m/z$  439.1 (Figure 3, Figure S10 of the Supporting Information).

All structures shown in Figure 2 were confirmed by HRMS analysis. In addition, when **1b** was used instead of **1a**,  $[\text{Pd}(\text{1-H})(\text{DMSO})_2]^+$ ,  $[\text{Pd}(\text{1})(\text{DMSO})_2\text{H}]^+$ ,  $[\text{Pd}(\text{1-H})_2(\text{BQ})\text{H}]^+$

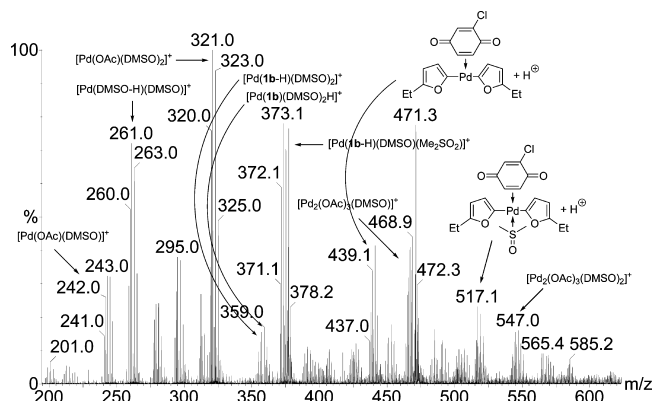


**Figure 3.** ESI(+)-MS of an AcOH/DMSO solution of **1b**, Pd(OAc)<sub>2</sub>, and Cl-BQ after 5 min. Conditions: **1b** (2.0 mmol), Pd(OAc)<sub>2</sub> (0.05 mmol), Cl-BQ (2.0 mmol), AcOH (2.0 mL), and DMSO (2.0 mL). *t<sub>R</sub>* = 5 min.

(DMSO)H]<sup>+</sup>, and [Pd<sub>2</sub>(**1-H**)(OAc)<sub>2</sub>(DMSO)]<sup>+</sup> were shifted by 14 or 28 mass units depending on the number of furyl ligands (Table 3, Figure S11 of the Supporting Information). It

**Table 3.** Comparison of Detected Species Using **1a** or **1b**

proposed structures	<i>m/z</i> observed with	
	<b>1a</b>	<b>1b</b>
[Pd( <b>1-H</b> )(DMSO) <sub>2</sub> ] <sup>+</sup>	343.0	357.1
[Pd( <b>1</b> )(DMSO) <sub>2</sub> H] <sup>+</sup>	345.0	359.1
[Pd( <b>1-H</b> ) <sub>2</sub> (BQ)(DMSO)H] <sup>+</sup>	455.0	483.2
[Pd <sub>2</sub> ( <b>1-H</b> )(OAc) <sub>2</sub> (DMSO)] <sup>+</sup>	488.9	503.1
[Pd <sub>2</sub> ( <b>1-H</b> )(OAc) <sub>2</sub> (DMSO) <sub>2</sub> ] <sup>+</sup>	566.9	—

was difficult to confirm the presence of [Pd<sub>2</sub>(**1b-H**)(OAc)<sub>2</sub>(DMSO)<sub>2</sub>]<sup>+</sup> due to the complexity of the spectrum in the range of *m/z* 560–600. The desolvated complex [Pd(**1b-H**)<sub>2</sub>(BQ)H]<sup>+</sup> was observed at *m/z* 405.2, and two new species at *m/z* 373.1 and 451.2 were identified as [Pd(**1b-H**)(DMSO)(Me<sub>2</sub>SO<sub>2</sub>)]<sup>+</sup> and [Pd(**1b-H**)(DMSO)<sub>2</sub>(Me<sub>2</sub>SO<sub>2</sub>)]<sup>+</sup>, respectively, by HRMS. Finally, only two clusters at *m/z* 413.0 and 425.0 could not be identified in Figure 2.

A mixture of Pd(OAc)<sub>2</sub>, BQ, and **1a** in AcOH/DMSO (1:1) was stirred for 5 min; **2a** was added, and the ESI(+)-MS was monitored after 5 min of additional stirring. Despite the low intensity of the signal, a cluster was identified at *m/z* 371.0 as [Pd(**2a-H**)(OAc)(DMSO)H]<sup>+</sup> (Figure 4, Figure S12 of the Supporting Information). The ESI(+)-MS/MS of [Pd(**2a-H**)(OAc)(DMSO)H]<sup>+</sup> showed the loss of DMSO, AcOH, and C<sub>4</sub>H<sub>8</sub> (Table 4, Figure S13 of the Supporting Information). The latter confirms the presence of a *tert*-butyl group. It must be noted that the MS/MS did not show the loss of **2a**, suggesting that the alkene is bound to the palladium center through a  $\sigma$  bond. Therefore, the corresponding neutral species, Pd(**2a-H**)(OAc)(DMSO), would result from the C–H activation of **2a** with mononuclear Pd(II) complexes. Such activation is generally not proposed or discussed in the mechanism of DHRs.

Two clusters, relatively close to each other, at *m/z* 393.1 and 395.1, were attributed to [Pd(**3aa+H**)(DMSO)]<sup>+</sup> and [Pd(**1a-H**)(**3aa**)]<sup>+</sup>, respectively (Figure 4, Figure S12 of the Supporting Information). The latter was also observed as the solvated species, [Pd(**1a-H**)(**3aa**)(DMSO)]<sup>+</sup>, at *m/z* 473.1. The signal was contaminated with another complex at *m/z* 475, which

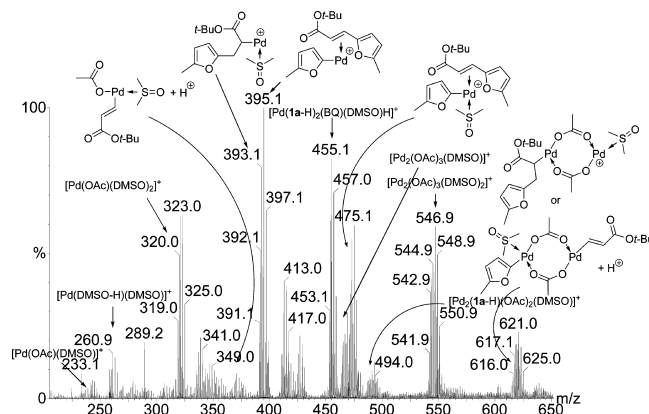


**Figure 4.** ESI(+)-MS of an AcOH/DMSO solution of **1a**, **2a**, Pd(OAc)<sub>2</sub>, and BQ after 10 min. Conditions: **1a** (2.0 mmol), **2a** (1.0 mmol), Pd(OAc)<sub>2</sub> (0.05 mmol), BQ (2.0 mmol), AcOH (2.0 mL), and DMSO (2.0 mL). *t<sub>R</sub>* = 10 min.

**Table 4.** ESI(+)-MS/MS of Detected Species for the Coupling of **1a** with **2a**

proposed structures	losses
[Pd( <b>2a-H</b> )(OAc)(DMSO)H] <sup>+</sup>	DMSO, AcOH, C <sub>4</sub> H <sub>8</sub>
[Pd( <b>3aa+H</b> )(DMSO)] <sup>+</sup>	DMSO, C <sub>4</sub> H <sub>8</sub>
[Pd( <b>1a-H</b> )( <b>3aa</b> )(DMSO)] <sup>+</sup>	DMSO, C <sub>4</sub> H <sub>8</sub> , <b>3aa</b>
[Pd <sub>2</sub> ( <b>3aa+H</b> )(OAc) <sub>2</sub> (DMSO)] <sup>+</sup> or [Pd <sub>2</sub> ( <b>1a-H</b> )( <b>2a-H</b> )(OAc) <sub>2</sub> (DMSO)H] <sup>+</sup>	DMSO, AcOH, Pd, C <sub>4</sub> H <sub>8</sub> , CH <sub>3</sub> CO <sub>2</sub> - <i>t</i> -Bu

according to the HRMS results, could be attributed to [Pd(**1a**)(**3aa**)(DMSO)H]<sup>+</sup>. However, the corresponding ESI(+)-MS/MS did not show the loss of **1a** and **3aa** as expected, and the hypothesis could not be confirmed. [Pd(**3aa+H**)(DMSO)]<sup>+</sup> dissociated to produce DMSO and C<sub>4</sub>H<sub>8</sub> (Table 4, Figure S14 of the Supporting Information). The corresponding neutral species, Pd(**3aa+H**)(OAc)(DMSO), resulted from the insertion of **2a** into the furyl–Pd(II) bond of Pd(**1a-H**)(OAc)(DMSO)<sub>2</sub> as generally proposed for the second step of the DHR. The ESI(+)-MS/MS of [Pd(**1a-H**)(**3aa**)(DMSO)]<sup>+</sup> has shown the loss of DMSO and C<sub>4</sub>H<sub>8</sub>. In addition, the elimination of **3aa** was observed, which confirms the coordination of the product to the palladium center (Table 4, Figure S15 of the Supporting Information). The corresponding neutral complex Pd(**1a-H**)(**3aa**)(OAc)(DMSO) could result from the coordination of **3aa** to Pd(**1a-H**)(OAc)(DMSO)<sub>2</sub>. Indeed, the ESI(+)-MS monitoring of an AcOH/DMSO solution of Pd(OAc)<sub>2</sub>, BQ, **3aa**, and **1a** has shown that **3aa** acts as a ligand of furyl–Pd(II) complexes. After 5 min of stirring, in addition to the clusters previously detected in the absence of **3aa** (Figures 1 and 2), two clusters were observed at *m/z* 395.2 and 473.2 that were above attributed to [Pd(**1a-H**)(**3aa**)]<sup>+</sup> and [Pd(**1a-H**)(**3aa**)(DMSO)]<sup>+</sup>, respectively (Figure 5, Figure S16 of the Supporting Information).

Finally, another cluster was detected at *m/z* 617.0 (Figure 4, Figure S12 of the Supporting Information) and attributed to [Pd<sub>2</sub>(**3aa+H**)(OAc)<sub>2</sub>(DMSO)]<sup>+</sup> or [Pd<sub>2</sub>(**1a-H**)(**2a-H**)(OAc)<sub>2</sub>(DMSO)H]<sup>+</sup> (Scheme 6). The ESI(+)-MS/MS of such species has shown the loss of DMSO, AcOH, Pd, and C<sub>4</sub>H<sub>8</sub> (Table 4, Figure S17 of the Supporting Information). Out of the two possible structures, [Pd<sub>2</sub>(**3aa+H**)(OAc)<sub>2</sub>(DMSO)]<sup>+</sup> or [Pd<sub>2</sub>(**1a-H**)(**2a-H**)(OAc)<sub>2</sub>(DMSO)H]<sup>+</sup>, the first seems the most probable with the loss of a *tert*-butyl acetate (*m/z* 116) (Table 4, Figure S17 of the Supporting Information).



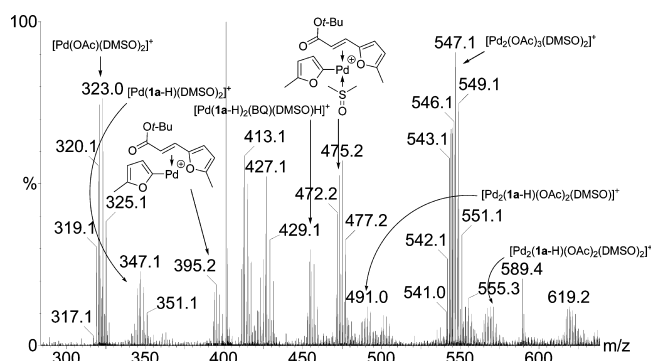


**Figure 5.** ESI(+)-MS of an AcOH/DMSO solution of **1a**, **3aa**, Pd(OAc)<sub>2</sub>, and BQ after 5 min. Conditions: **1a** (2.0 mmol), **3aa** (0.5 mmol), Pd(OAc)<sub>2</sub> (0.05 mmol), BQ (2.0 mmol), AcOH (2.0 mL), and DMSO (2.0 mL). *t<sub>R</sub>* = 5 min.

The corresponding neutral dinuclear species, Pd<sub>2</sub>(**3aa**+H)-(OAc)<sub>3</sub>(DMSO), could result from the insertion of **2a** into the furyl bond of Pd<sub>2</sub>(**1a**-H)(OAc)<sub>3</sub>(DMSO). The other possible dinuclear complex Pd<sub>2</sub>(**1a**-H)(**2a**-H)(OAc)<sub>2</sub>(DMSO) could be associated with the complexation of both mononuclear species, Pd(**1a**-H)(OAc)(DMSO)<sub>2</sub> and Pd(**2a**-H)(OAc)(DMSO), or the C–H activation of **2a** by Pd<sub>2</sub>(**1a**-H)(OAc)<sub>3</sub>(DMSO). The double C–H activation of arenes and alkenes by palladium(II), which would be followed by a reductive elimination to obtain the product, has been discussed in the early studies of the DHRs.<sup>24</sup> It has even been proposed that the rate-determining step could correspond to the formation of the σ-bond between palladium and olefin.<sup>24b</sup> However, the comparison of the Pd(II)-catalyzed reactivity of PhH toward PhCH=CD<sub>2</sub> and PhCH=CH<sub>2</sub> led to the suggestion that the cleavage of the styrene β-hydrogen bond is not involved in the rate-determining step.<sup>25</sup> According to subsequent studies, it appears that the formation of the ArPd(II) species from CH<sub>2</sub>=CHR/ArH/Pd(OAc)<sub>2</sub> mixtures occurred at the rate-determining step.<sup>1</sup> However, it should be noted that the detection by ESI-MS(+) of [Pd(**2a**-H)(OAc)(DMSO)H]<sup>+</sup> suggests that the C–H activation of **2a** by Pd(II) is probable and can play a role in the mechanism.

All structures shown in Figure 4 agreed with the HRMS analysis. In addition, using ESI(+)-MS, the monitoring of the coupling of **1b** with **2a** and **1a** with ethyl acrylate (**2b**) showed shifts of 14 or 28 amu as expected, except for [Pd(**2b**-H)(OAc)(DMSO)H]<sup>+</sup> that has a mass close to that of [Pd(**1a**-H)(DMSO)<sub>2</sub>]<sup>+</sup><sup>26</sup> and [Pd<sub>2</sub>(**3ab**+H)(OAc)<sub>2</sub>(DMSO)]<sup>+</sup>/[Pd<sub>2</sub>(**1a**-H)(**2b**-H)(OAc)<sub>2</sub>(DMSO)H]<sup>+</sup>, which could not be

confirmed due to the complexity of the spectra (Table 5, Figures S18 and S19 of the Supporting Information). The cluster at *m/z* 481 in Figure S19 of the Supporting Information could not be identified.

**Table 5.** Comparison of Detected Species for the Coupling of **1a** with **2a**, **1b** with **2a**, and **1a** with **2b**

proposed structures	<i>m/z</i> observed for the coupling of		
	<b>1a</b> with <b>2a</b>	<b>1b</b> with <b>2a</b>	<b>1a</b> with <b>2b</b>
[Pd( <b>2</b> -H)(OAc)(DMSO)H] <sup>+</sup>	371.0	371.0	–
[Pd( <b>3</b> +H)(DMSO)] <sup>+</sup>	393.1	407.2	365.1
[Pd( <b>1</b> -H)( <b>3</b> )] <sup>+</sup>	395.1	423.2	367.3
[Pd( <b>1</b> -H)( <b>3</b> )(DMSO)] <sup>+</sup>	473.1	501.3	445.2
[Pd <sub>2</sub> ( <b>3</b> +H)(OAc) <sub>2</sub> (DMSO)] <sup>+</sup> or [Pd <sub>2</sub> ( <b>1</b> -H)( <b>2</b> -H)(OAc) <sub>2</sub> (DMSO)H] <sup>+</sup>	617.0	631.4	–

The monitoring of the coupling of **1a** with **2a** by ESI(+)-MS was pursued over 24 h. After 2.5 h, the abundance of most identified clusters has decreased (Figure 6, Figure S20 of the

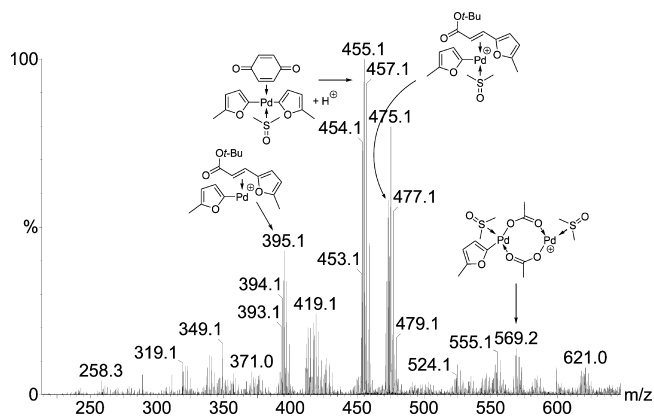
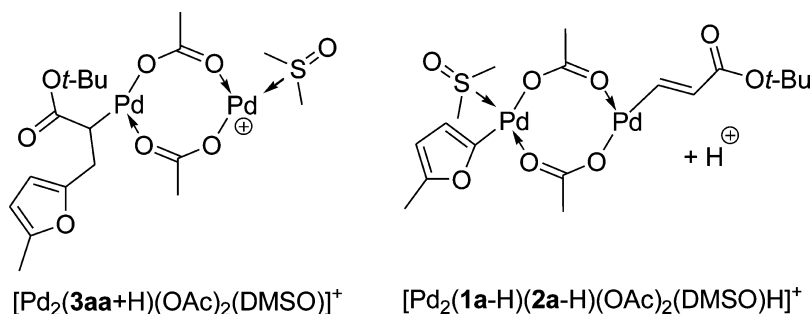


**Figure 6.** ESI(+)-MS of an AcOH/DMSO solution of **1a**, **2a**, Pd(OAc)<sub>2</sub>, and BQ after 2.5 h. Conditions: **1a** (2.0 mmol), **2a** (1.0 mmol), Pd(OAc)<sub>2</sub> (0.05 mmol), BQ (2.0 mmol), AcOH (2.0 mL), and DMSO (2.0 mL). *t<sub>R</sub>* = 2.5 h.

Supporting Information). The remaining species are connected to the C–H activation of **1a** or to the coordination of **3aa** to the palladium center. This is consistent with the fact that **1a** is used in excess, and that the reaction is almost complete after 2.5 h as observed by GC.

#### Scheme 6. Proposed Structures for the Cluster Detected at *m/z* 617.0<sup>a</sup>



<sup>a</sup>Isomers are not represented for clarity.

After 24 h, the ESI(+)-MS is quite complex and most signals have low intensity (Figure 7, Figure S21 of the Supporting

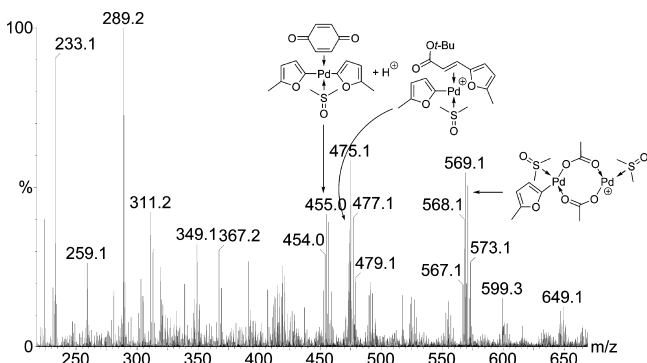


**Figure 7.** ESI(+)-MS of an AcOH/DMSO solution of **1a**, **2a**, Pd(OAc)<sub>2</sub>, and BQ after 24 h. Conditions: **1a** (2.0 mmol), **2a** (1.0 mmol), Pd(OAc)<sub>2</sub> (0.05 mmol), BQ (2.0 mmol), AcOH (2.0 mL), and DMSO (2.0 mL). *t<sub>R</sub>* = 24 h.

Information). As previously observed after 2.5 h, the most abundant clusters are connected to the C–H activation of **1a** or the coordination of **3aa** to the palladium center.

Given the results obtained from the ESI-MS study, the following mechanisms are proposed. The inactive trimer [Pd(OAc)<sub>2</sub>]<sub>3</sub>, **A**, reacts with DMSO leading to active dimer or monomer derivatives, **B** (Scheme 7). **B1** activates a C–H bond of DMSO and **2**, while **B1** and **B2** activate a C–H bond

of **1** leading to the furyl–Pd complexes, **C**. After a few catalytic cycles, **3** is present and, consequently, can act as a ligand of **C**. The insertion of **2** leads to **D**, which suffers β-hydride elimination to give **E**. Reductive elimination affords the Pd(0) complex, **F**, and reoxidation of Pd(0) by BQ/AcOH finishes the catalytic cycle.

With regard to the formation of **4**, complex **C** leads to **G** through the C–H activation of **1** (Scheme 8). The resulting electron-rich **G** coordinates BQ to give **H**, which evolves through reductive elimination to **4** and Pd(0). The latter is reoxidized by BQ/AcOH.

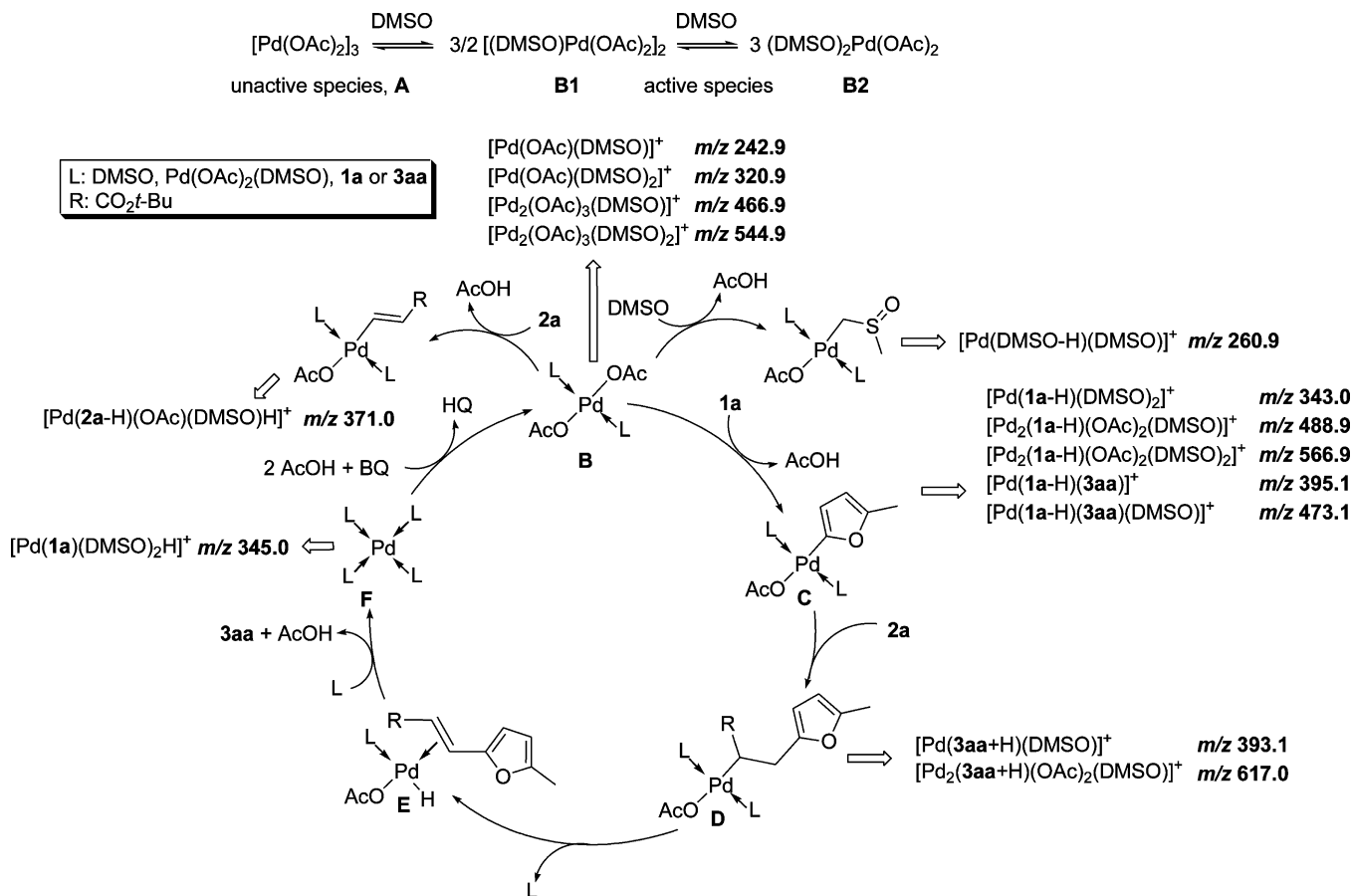
## CONCLUSION

Mechanistic proposals of DHRs usually involve mononuclear catalytic intermediates. Using ESI-MS in the present study, we show that dinuclear species can be involved. Mononuclear and dinuclear furyl–Pd(II) intermediates obtained through C–H activation and complexes resulting from the insertion of the alkene into the furyl–Pd(II) bond have been intercepted and characterized. Secondary reactions, such as the C–H activation of DMSO or the alkene, have been identified. An intermediate involved in the homocoupling of furans through C–H activation has also been detected and characterized. Moreover, it seems that the coordination of BQ to Pd is observed for the first time using ESI-MS.

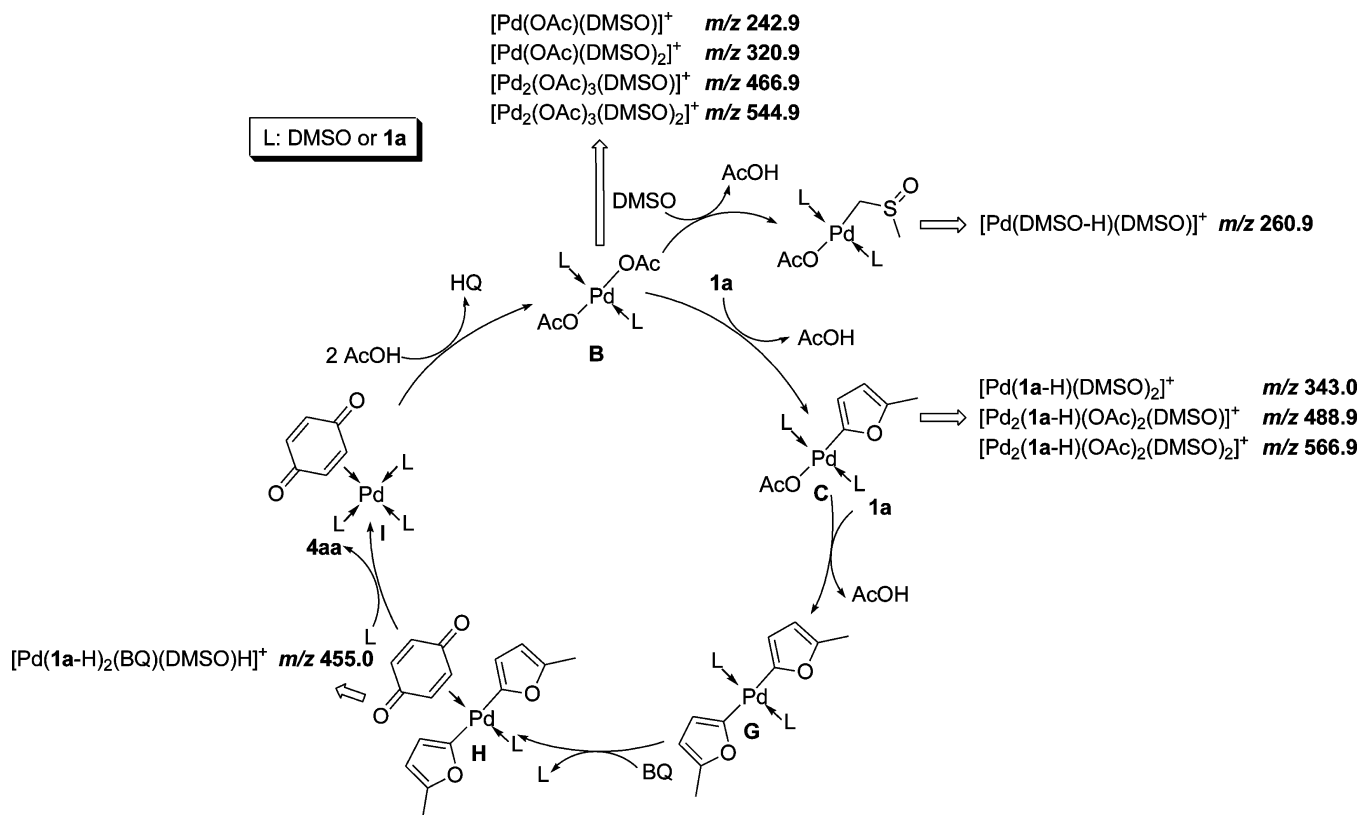
## EXPERIMENTAL SECTION

**General Information.** Solvents and reagents were used as received. Electrospray ionization-mass spectrometry experiments

**Scheme 7.** Proposed Catalytic Cycle and Species Detected by ESI(+)-MS for the DHR of **1a** with **2a**



Scheme 8. Proposed Catalytic Cycle and Species Detected by ESI(+)-MS for the Synthesis of 4aa



(MS and HRMS) were conducted on a hybrid tandem quadrupole-time of flight (Q-TOF) instrument, equipped with a pneumatically assisted electrospray (Z-spray) ion source. ALPHAGAZ AR2 gas was used for CID. The electrospray potential was set to 3 kV in positive ion mode, and the extraction cone voltage was usually varied between 30 and 60 V (flow of injection 5  $\mu$ L/min). Spectra were typically an average of 20–40 scans. Theoretical isotope patterns calculated with the Isoform program were used to aid in the assignment. In order to obtain a valid exact mass measurement, an external reference or “lock mass” was used to correct for changes in environment or experimental conditions over the course of the analysis. The LockSpray dual electrospray ion source optimizes the co-introduction of the analyte and lock mass compound directly into the ion source, providing an authenticated exact mass measurement in MS modes to within 5 ppm rms mass accuracy.

**General Procedure for ESI-MS Experiments.** BQ (216.0 mg, 2.0 mmol), Pd(OAc)<sub>2</sub> (11.2 mg, 0.05 mmol), DMSO (2.0 mL), and AcOH (2.0 mL) were added to a round-bottom flask. After the contents of the flask had been stirred for 5 min, **1** (2.0 mmol) and **2** (1.0 mmol) were added. The reaction mixture was directly injected into the ESI-MS spectrometer at regular intervals of time.

## ■ ASSOCIATED CONTENT

### ● Supporting Information

SHRMS data and Figures S1–S21. This material is available free of charge via the Internet at <http://pubs.acs.org>.

## ■ AUTHOR INFORMATION

### Corresponding Author

\*E-mail: [jean.lebras@univ-reims.fr](mailto:jean.lebras@univ-reims.fr). Fax: (+)33 3 26 91 31 66.

### Notes

The authors declare no competing financial interest.

## ■ ACKNOWLEDGMENTS

Financial support by CNRS, Conseil Régional Champagne Ardenne, Ministry of Higher Education and Research (MESR), and EU-programme FEDER to the PIAneT CPER project is gratefully acknowledged.

## ■ REFERENCES

- (1) Le Bras, J.; Muzart, J. *Chem. Rev.* **2011**, *111*, 1170–1214.
- (2) (a) Zhang, Y.; Li, Z.; Liu, Z.-Q. *Org. Lett.* **2012**, *14*, 226–229. (b) Shang, X.; Xiong, Y.; Zhang, Y.; Zhang, L.; Liu, Z. *Synlett* **2012**, 259–262. (c) Li, Z.; Zhang, Y.; Liu, Z.-Q. *Org. Lett.* **2012**, *14*, 74–77.
- (d) Fan, S.; Chen, F.; Zhang, X. *Angew. Chem., Int. Ed.* **2011**, *50*, 5918–5923.
- (3) Kubota, A.; Emmert, M. H.; Sanford, M. S. *Org. Lett.* **2012**, *14*, 1760–1763.
- (4) (a) Wang, L.; Guo, W.; Zhang, X.-X.; Xia, X.-D.; Xiao, W.-J. *Org. Lett.* **2012**, *14*, 740–743. (b) Zhu, C.; Falck, J. R. *Org. Lett.* **2011**, *13*, 1214–1217. (c) Wrighlesworth, J. W.; Cox, B.; Lloyd-Jones, G. C.; Booker-Milburn, K. I. *Org. Lett.* **2011**, *13*, 5326–5329. (d) Kim, B. S.; Lee, S. Y.; Youn, S. W. *Chem.—Asian J.* **2011**, *6*, 1952–1957. (e) Li, D.-D.; Yuan, T.-T.; Wang, G.-W. *Chem. Commun.* **2011**, *47*, 12789–12791.
- (5) Musaev, D. G.; Kaledin, A.; Shi, B.-F.; Yu, J.-Q. *J. Am. Chem. Soc.* **2012**, *134*, 1690–1698.
- (6) Kandukuri, S. R.; Schiffner, J. A.; Oestreich, M. *Angew. Chem., Int. Ed.* **2012**, *51*, 1265–1269.
- (7) (a) Chen, F.; Feng, Z.; He, C.-Y.; Wang, H.-Y.; Guo, Y.-L.; Zhang, X. *Org. Lett.* **2012**, *14*, 1176–1179. (b) Gandeepan, P.; Cheng, C.-H. *J. Am. Chem. Soc.* **2012**, *134*, 5738–5741. (c) Schmidt, B.; Elizarov, N. *Chem. Commun.* **2012**, *48*, 4350–4352. (d) Yu, M.; Xie, Y.; Xie, C.; Zhang, Y. *Org. Lett.* **2012**, *14*, 2164–2167. (e) Mizuta, Y.; Obora, Y.; Shimizu, Y.; Ishii, Y. *ChemCatChem* **2012**, *4*, 187–191. (f) Zhang, S.; Shi, L.; Ding, Y. *J. Am. Chem. Soc.* **2011**, *133*, 20218–20229. (g) Yu, M.; Liang, Z.; Wang, Y.; Zhang, Y. *J. Org. Chem.* **2011**, *76*, 4987–4994. (h) Ye, M.; Gao, G.-L.; Yu, J.-Q. *J. Am. Chem. Soc.* **2011**, *133*, 6964–



6967. (i) Wang, L.; Liu, S.; Li, Z.; Yu, Y. *Org. Lett.* **2011**, *13*, 6137–6139. (j) Wang, C.; Ge, H. *Chem.—Eur. J.* **2011**, *17*, 14371–14374. (k) Huang, C.; Chattopadhyay, B.; Gevorgyan, V. *J. Am. Chem. Soc.* **2011**, *133*, 12406–12409. (l) García-Rubia, A.; Urones, B.; Arrayás, R. G.; Carretero, J. C. *Angew. Chem., Int. Ed.* **2011**, *50*, 10927–10931. (m) García-Rubia, A.; Fernández-Ibáñez, M. Á.; Arrayás, R. G.; Carretero, J. C. *Chem.—Eur. J.* **2011**, *17*, 3567–3570.
- (8) (a) Santos, L. S. *Reactive Intermediates: MS Investigations in Solution*; Wiley-VCH: Weinheim, Germany, 2010. (b) Belyakov, P. A.; Kadentsev, V. I.; Chizhov, A. O.; Kolotyckina, N. G.; Shashkov, A. S.; Ananikov, V. P. *Mendeleev Commun.* **2010**, *20*, 125–131. (c) Müller, C. A.; Markert, C.; Teichert, A. M.; Pfaltz, A. *Chem. Commun.* **2009**, 1607–1618. (d) Chisholm, D. M.; Scott McIndoe, J. *Dalton Trans.* **2008**, 3933–3945. (e) Santos, L. S. *Eur. J. Org. Chem.* **2008**, 235–253. (f) Eberlin, M. N. *Eur. J. Mass Spectrom.* **2007**, *13*, 19–28. (g) Chen, P. *Angew. Chem., Int. Ed.* **2003**, *42*, 2832–2847.
- (9) (a) Sabino, A. A.; Machado, A. H. L.; Correia, C. R. D.; Eberlin, M. N. *Angew. Chem., Int. Ed.* **2004**, *43*, 2514–2518. (b) Santos, L. S.; Pavam, C. H.; Almeida, W. P.; Coelho, F.; Eberlin, M. N. *Angew. Chem., Int. Ed.* **2004**, *43*, 4330–4333.
- (10) (a) Wang, H.-Y.; Yim, W.-L.; Guo, Y.-L.; Metzger, J. O. *Organometallics* **2012**, *31*, 1627–1634. (b) Vikse, K. L.; Ahmadi, Z.; Manning, C. C.; Harrington, D. A.; McIndoe, J. S. *Angew. Chem., Int. Ed.* **2011**, *50*, 8304–8306. (c) Regiani, T.; Santos, V. G.; Godoi, M. N.; Vaz, B. G.; Eberlin, M. N.; Coelho, F. *Chem. Commun.* **2011**, 47, 6593–6595. (d) Oliveira, F. F. D.; dos Santos, M. R.; Lalli, P. M.; Schmidt, E. M.; Bakuzis, P.; Lapis, A. A. M.; Monteiro, A. L.; Eberlin, M. N.; Neto, B. A. D. *J. Org. Chem.* **2011**, *76*, 10140–10147. (e) Henderson, M. A.; Luo, J.; Oliver, A.; McIndoe, J. S. *Organometallics* **2011**, *30*, 5471–5479. (f) Alachraf, M. W.; Handayani, P. P.; Hüttel, M. R. M.; Grondal, C.; Enders, D.; Schrader, W. *Org. Biomol. Chem.* **2011**, *9*, 1047–1053. (g) Vikse, K. L.; Henderson, M. A.; Oliver, A. G.; McIndoe, J. S. *Chem. Commun.* **2010**, 46, 7412–7414. (h) Schade, M. A.; Fleckenstein, J. E.; Knochel, P.; Koszinowski, K. *J. Org. Chem.* **2010**, *75*, 6848–6857. (i) Fernandes, T. A.; Vaz, B. G.; Eberlin, M. N.; da Silva, A. J. M.; Costa, P. R. R. *J. Org. Chem.* **2010**, *75*, 7085–7091. (j) Beierlein, C. H.; Breit, B.; Paz Schmidt, R. A.; Plattner, D. A. *Organometallics* **2010**, *29*, 2521–2532. (k) Amarante, G. W.; Milagre, H. M. S.; Vaz, B. G.; Ferreira, B. R. V.; Eberlin, M. N.; Coelho, F. *J. Org. Chem.* **2009**, *74*, 3031–3037. (l) Amarante, G. W.; Benassi, M.; Milagre, H. M. S.; Braga, A. A. C.; Maseras, F.; Eberlin, M. N.; Coelho, F. *Chem.—Eur. J.* **2009**, *15*, 12460–12469. (m) Santos, L. S.; Rosso, G. B.; Pilli, R. A.; Eberlin, M. N. *J. Org. Chem.* **2007**, *72*, 5809–5812. (n) Markert, C.; Neuburger, M.; Kulicke, K.; Meuwly, M.; Pfaltz, A. *Angew. Chem., Int. Ed.* **2007**, *46*, 5892–5895. (o) Marquez, C. A.; Fabbretti, F.; Metzger, J. O. *Angew. Chem., Int. Ed.* **2007**, *46*, 6915–6917. (p) Thiery, E.; Chevrin, C.; Le Bras, J. *J. Org. Chem.* **2007**, *72*, 1859–1862.
- (11) Aouf, C.; Thiery, E.; Le Bras, J.; Muzart, J. *Org. Lett.* **2009**, *11*, 4096–4099.
- (12) Thiery, E.; Harakat, D.; Le Bras, J.; Muzart, J. *Organometallics* **2008**, *27*, 3996–4004.
- (13) Risberg, E. D.; Mink, J.; Abbasi, A.; Skripkin, M. Y.; Hajba, L.; Lindqvist-Reis, P.; Bencze, E.; Sandström, M. *Dalton Trans.* **2009**, 1328–1338.
- (14) Vasseur, A.; Muzart, J.; Le Bras, J. *Chem.—Eur. J.* **2011**, *17*, 12556–12560.
- (15) Skapski, A. C.; Smart, M. L. *J. Chem. Soc., Chem. Commun.* **1970**, 658–659.
- (16) Kurzev, S. A.; Kazankov, G. M.; Ryabov, A. D. *Inorg. Chim. Acta* **2002**, *340*, 192–196.
- (17) Boutadla, Y.; Davies, D. L.; Macgregor, S. A.; Poblador-Bahamonde, A. I. *Dalton Trans.* **2009**, 5820–5831.
- (18) DMSO is an ambidentate ligand that can bind to metal centers either through the sulfur or through the oxygen atom. It has been shown by computational studies that S-bound or O-bound DMSO is the preferable coordination mode of palladium(II) depending on the ligand environment, while palladium(0) prefers mainly S-bound DMSO. See: Zierkiewicz, W.; Privalov, T. *Organometallics* **2005**, *24*, 6019–6028.
- (19) The reduction could occur during the desolvation step.
- (20) The fragmentation of  $[\text{Pd}(\mathbf{1a-H})(\text{DMSO})_2]^+$  and  $[\text{Pd}(\mathbf{1a})(\text{DMSO})_2\text{H}]^+$  has shown the loss of 60 amu, which could be interpreted as the dissociation of AcOH. However, this loss was also observed when  $\text{CD}_3\text{CO}_2\text{D}$  was used as solvent and probably comes from the fragmentation of **1a** or DMSO.
- (21) (a) Albéniz, A. C.; Espinet, P.; Martín-Ruiz, B. *Chem.—Eur. J.* **2001**, *11*, 2481–2489. (b) Chen, X.; Li, J. J.; Hao, X.-S.; Goodhue, C. E.; Yu, J.-Q. *J. Am. Chem. Soc.* **2006**, *128*, 78–79. (c) Pérez-Rodríguez, M.; Braga, A. A. C.; García-Melchor, M.; Pérez-Temprano, M. H.; Casares, J. A.; Ujacque, G.; de Lera, A. R.; Álvarez, R.; Maseras, F.; Espinet, P. *J. Am. Chem. Soc.* **2009**, *131*, 3650–3657. (d) Hull, K. L.; Sanford, M. S. *J. Am. Chem. Soc.* **2009**, *131*, 9651–9653.
- (22) Qian, R.; Guo, Y.; Lü, L. *Chin. J. Chem.* **2008**, *26*, 123–129.
- (23) Harakat, D.; Muzart, J.; Le Bras, J. *RSC Adv.* **2012**, *2*, 3094–3099.
- (24) (a) Danno, S.; Moritani, I.; Fujiwara, Y. *Tetrahedron* **1969**, *25*, 4819–4823. (b) Fujiwara, Y.; Moritani, I.; Asano, R.; Tanaka, H.; Teranishi, S. *Tetrahedron* **1969**, *25*, 4815–4818. (c) Danno, S.; Moritani, I.; Fujiwara, Y.; Teranishi, S. *J. Chem. Soc. B* **1971**, 196–198.
- (25) Shue, R. S. *J. Am. Chem. Soc.* **1971**, *93*, 7116–7117.
- (26) If the presence of  $[\text{Pd}(\mathbf{2b-H})(\text{OAc})(\text{DMSO})\text{H}]^+$  could not be confirmed, it should be noted that the signal at  $m/z$  371 attributed to  $[\text{Pd}(\mathbf{2a-H})(\text{OAc})(\text{DMSO})\text{H}]^+$  was not observed when **2b** was used as an alkene.